Estimation of Surface Rain Rates from TEMPEST STP-H8 Brightness Temperature Observations using Machine Learning

Chandrasekar Radhakrishnan[1], V. Chandrasekar[1], Steven C. Reising[1] and Shannon T. Brown[2]

Eun Yeol[1] (Presenter)

[1]Electrical and Computer Engineering, Colorado State University, Fort Collins, CO, USA
[2]Jet Propulsion Laboratory, California Institute of Technology, Pasadena, CA, USA

11th Workshop of International Precipitation Working Group (IPWG-11)

Tokyo Institute of Technology, Tokyo, Japan

15-18 July 2024

Jet Propulsion Laboratory
California Institute of Technology

Overview and Objectives

- The objective of this research is to estimate surface rain rates using observations performed by the Temporal Experiment for Storms and Tropical Systems (TEMPEST) Space Test Program-Houston 8 (STP-H8).
- A machine learning based surface rainfall estimation system is developed from TEMPEST-D Brightness Temperature (TB) observations.
- The machine learning algorithms employ a combination of Random Forest (RF) classification and regression techniques.
- Rain rate products from the Global Precipitation Measurement (GPM) Microwave Imager (GMI) and Advanced Microwave Scanning Radiometer 2 (AMSR2) are used as reference data in the machine learning algorithms.

Temporal Experiment for Storms and Tropical systems – Demonstration (TEMPEST-D) Mission

- TEMPEST-D mission [1] is a NASA Earth Venture Technology Demonstration mission to demonstrate the technology necessary to perform high temporal-resolution observations of clouds, convection and water vapor profiles from small satellites.
- TEMPEST-D is a collaboration among CSU, NASA/JPL and Blue Canyon Technologies.
- TEMPEST-D is a 6U CubeSat with a cross-track scanning millimeter-wave radiometer observing the Earth at 87, 164, 174, 178 and 181 GHz.

- Spatial resolution varies from 25 km at 87 GHz to 12.5 km at 164-181 GHz.
- Originally planned for a 3-month technology demonstration, TEMPEST-D performed well-calibrated and highly stable global atmospheric observations for nearly 3 years. (between September 2018 and May 2021)

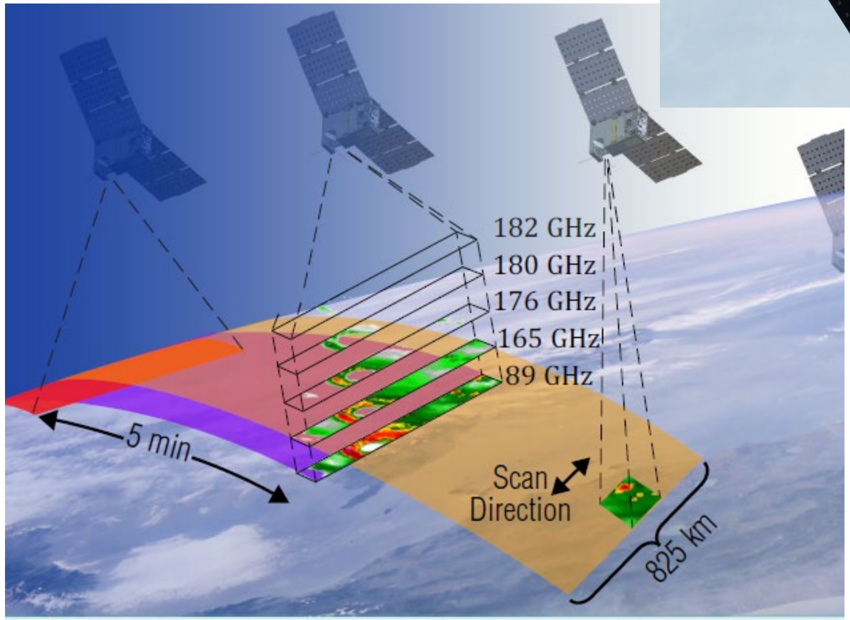

Temporal Experiment for Storms and Tropical Systems (TEMPEST) Space Test Program-Houston 8 (STP-H8)

- The TEMPEST STP-H8 sensor is nearly identical to the TEMPEST-D instrument, with slight differences in channel center frequencies and spectral responses.
- TEMPEST STP-H8 performs TB observations at five millimeter-wave frequencies of 89, 165, 176, 180, and 182 GHz and has been providing nearly continuous measurements from the ISS since January 8, 2022.
- The machine learning rain rate estimation system developed using TEMPEST-D TB observations has been applied to estimate the rain rate from TEMPEST STP-H8 TB observations.

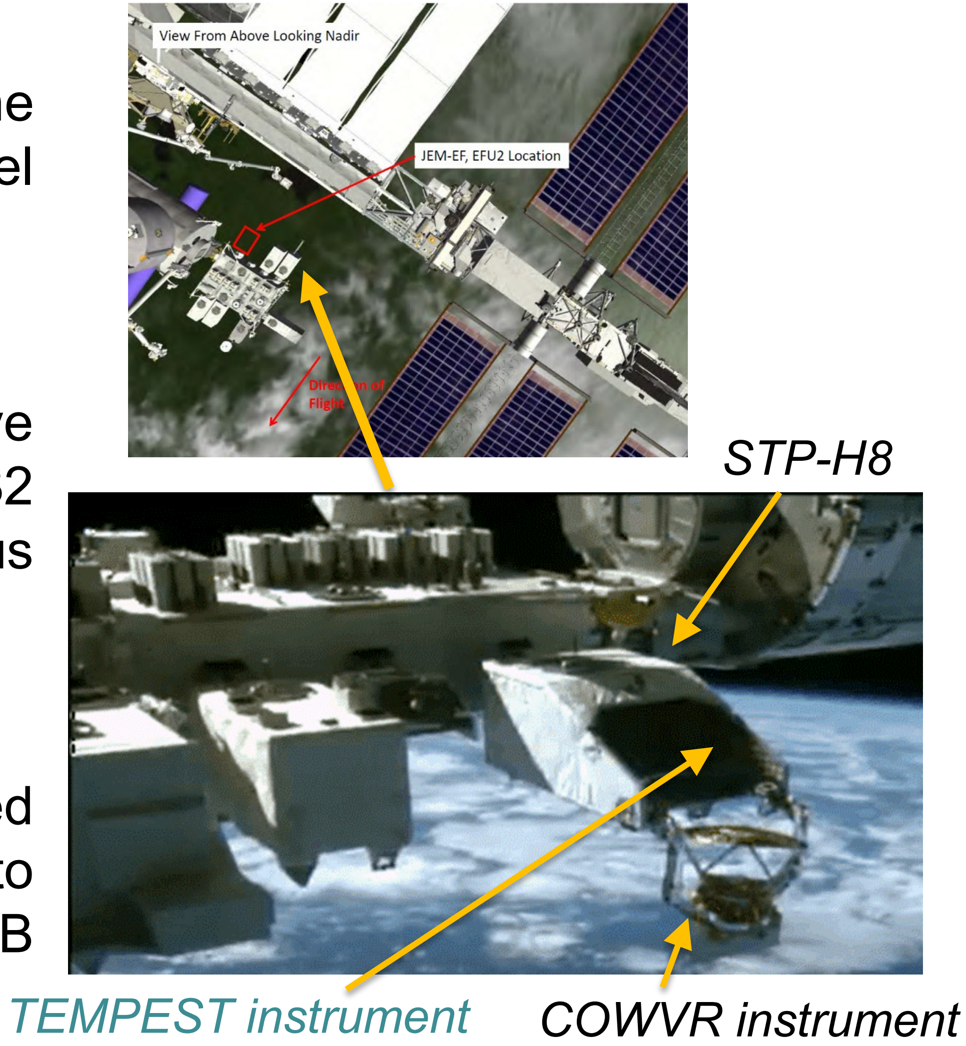

Image source : https://space.skyrocket.de/doc_sdat/stp-h8.htm

TEMPEST-D Observations over Tropical Cyclones

Hurricane Florence
on September 11, 2018

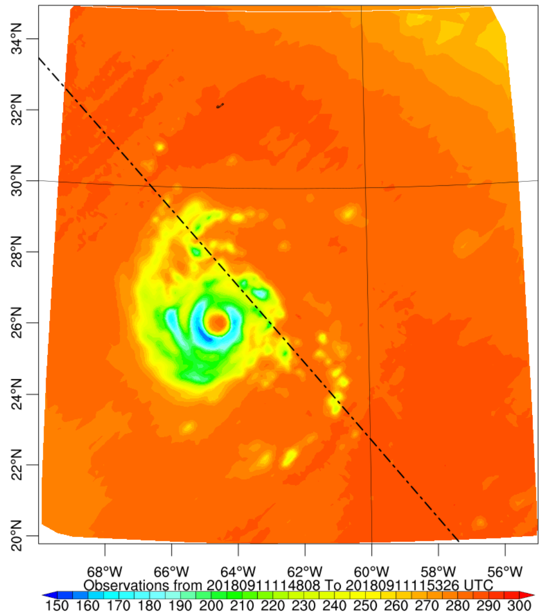

Atlantic Ocean

Hurricane Juliette
on September 5, 2019

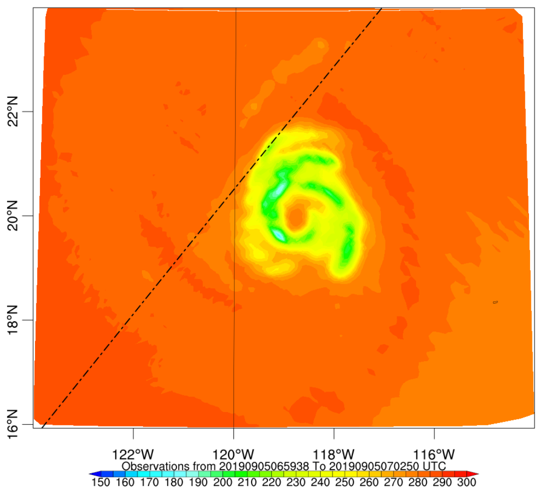

Eastern Pacific Ocean

Tropical Cyclone Nisarga
on June 3, 2020

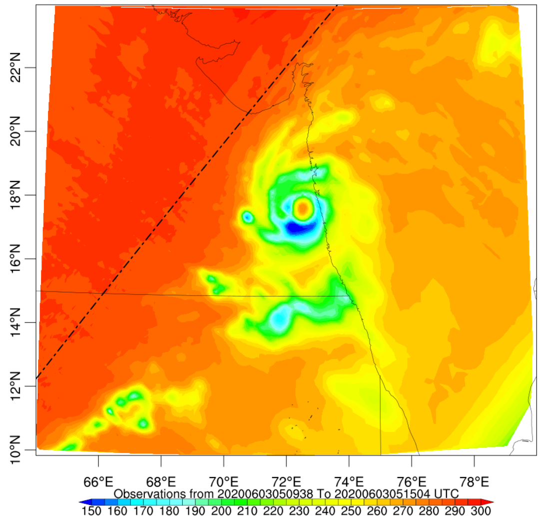

Indian Ocean

Typhoon Surigae
on April 16, 2021

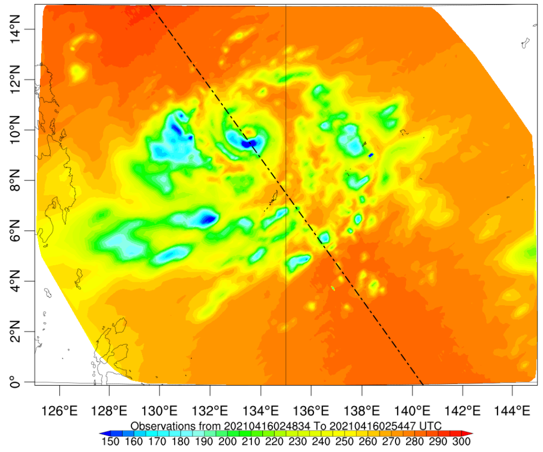

Western Pacific Ocean

TEMPEST-D 164 GHz Brightness Temperature (K) Images

Cross-Validation of TEMPEST-D and GPM-GMI Observations

Comparison of NOAA best track with combined storm tracks from TEMPEST-D and GPM-GMI

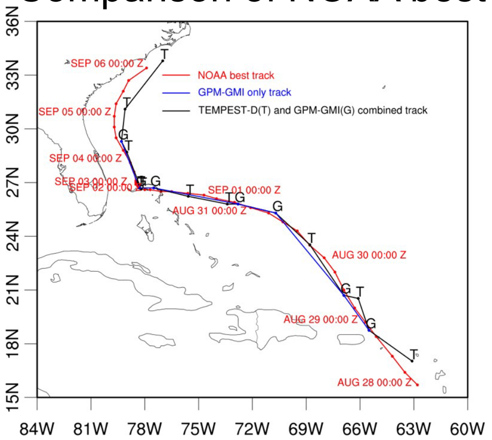

Hurricane Dorian (2019)

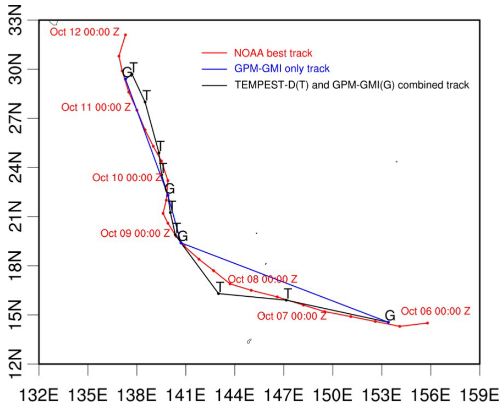

Typhoon Hagibis (2019)

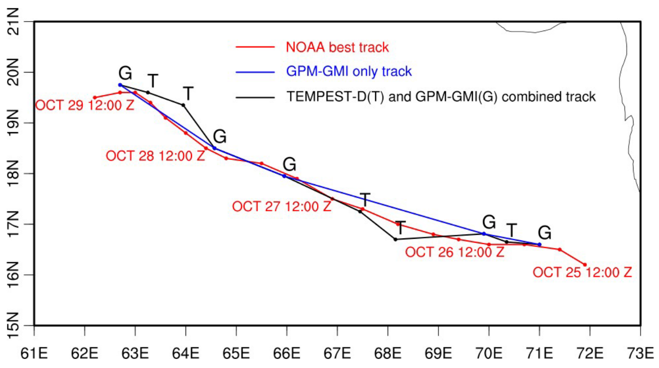

Tropical Cyclone Kyarr (2019)

- TEMPEST-D brightness temperature observations were validated over precipitating systems on a global basis. TEMPEST-D (164 GHz) and GPM-GMI (166 GHz horizontal and vertical channel) brightness temperature observations, with different sensor properties and viewing geometries, have a mean absolute difference of 2.9 K. The correlation coefficient between TEMPEST-D and GPM-GMI brightness temperatures is 0.86.
- When combined with GMI, TEMPEST-D increases the temporal sampling frequency of TCs by a factor of approximately 2.5.

7422 IEEE JOURNAL OF SELECTED TOPICS IN APPLIED EARTH OBSERVATIONS AND REMOTE SENSING, VOL. 16, 2023

TEMPEST-D and GPM-GMI Observations Over Precipitating Systems: A Cross-Validation Study

Chandrasekar Radhakrishnan, V. Chandrasekar, *Fellow, IEEE*, Steven C. Reising, *Senior Member, IEEE*, Wesley Berg, and Shannon T. Brown, *Senior Member, IEEE*

Abstract—The objective of this study is to cross-validate observations over precipitating systems by microwave radiometers on the temporal experiment for storms and tropical systems demonstration (TEMPEST-D) CubeSat mission and the global precipitation measurement microwave imager (GMI). The purpose of this article is twofold: first, to show consistency between TEMPEST-D and GMI observations, and second, to demonstrate the potential to enhance temporal sampling when TEMPEST-D and GMI observations are merged. Two cross-validation methodologies were employed. The first cross-validation methodology is to quantitatively compare TEMPEST-D and GMI brightness temperature (TB) observations over precipitation systems using a priori spatiotemporal constraints. The comparative analysis showed that the two instruments' TB observations have similar probability distributions, with a mean absolute difference of 2.9 K. The second cross-validation methodology is to quantitatively compare TEMPEST-D and GMI TB observations over tropical cyclone systems. Three storm cases were analyzed in this comparative study. The analysis showed that the structure and intensity of the storms are similar in TEMPEST-D and GMI TB observations, and the overall average correlation coefficient (r) is 0.9. Combining TEMPEST-D and GMI TB observations over the hurricane systems increased the sampling frequency by a factor of 2.5, compared to using the GMI data alone.

Index Terms—Brightness temperature (TB), CubeSat, global microwave imager, global precipitation mission, hurricane, microwave radiometer, temporal experiment for storms and tropical systems demonstration (TEMPEST-D), tropical cyclone, typhoon.

I. INTRODUCTION

THE knowledge of precipitation over land and the world's oceans is essential to understand the development and evolution of oceanic storms, especially cyclonic storms that may make landfall and cause damage to life and property. Weather satellites are a critical part of the infrastructure used to monitor storms over the world's oceans. Passive microwave (PMW) sensors have a long heritage of performing observations over convective storms. Even though PMW sensors have been shown to be very useful, they are currently available only in low Earth orbit (LEO) [1], [2], [3]. Therefore, they have limited temporal resolution compared to visible and Infrared sensors in geostationary orbit satellites as well as ground-based radar observations. High temporal resolution observations on time scales of tens of minutes are needed to monitor the evolution of storms for various applications, including storm tracking and prediction of intensity. Recent use of CubeSat and small satellite technology has provided a viable and cost-effective approach to observe storms and precipitation systems at a reasonable temporal resolution using satellite constellations. Kulu et al. [4] reported that as of August 1, 2022, more than 1897 CubeSats had been successfully deployed in LEO. Goncharenko et al. [5] analyzed CubeSat constellations and demonstrated their capability of reducing average revisit time at a reasonable cost. Observations from new microwave radiometric sensors need to be cross validated and calibrated before ingesting them into operational weather models and combining them with other satellite observations to generate global weather products. A number of studies have been conducted for validation of CubeSat brightness temperature (TB) observations and cross comparison with other satellite observations. Schulte et al. [6] used the Colorado State University one-dimensional variational retrieval algorithm to retrieve total precipitable water, cloud liquid water path, and cloud ice water path from the temporal experiment for storms and tropical systems demonstration (TEMPEST-D) and microwave humidity sounder (MHS) observations. The retrievals showed that TEMPEST-D has similar performance to the larger MHS on traditional MetOp satellites. Validation of TEMPEST-D observations through cross calibration with scientific and operational satellite sensors [7] showed that even though TEMPEST-D is a 6U CubeSat (20 cm × 10 cm × 34 cm dimensions), it has performed science-quality observations. The TEMPEST-D radiometer has similar or better performance to large satellites in terms of calibration accuracy, instrument noise, and calibration stability or precision. Chandrasekar et al. [8] and Radhakrishnan et al. [9] cross validated TEMPEST-D and RainCube CubeSat observations. This study showed that even though these two microwave instruments are heterogeneous, i.e., RainCube is an active radar and TEMPEST-D is a microwave

Manuscript received 7 April 2023; revised 18 May 2023 and 12 July 2023; accepted 28 July 2023. Date of publication 4 August 2023; date of current version 15 August 2023. This work was supported by the NASA Earth Venture Technology Demonstration Program under Grant NNX15AP56G, Grant 80NSSC20K1124, and Grant 80NSSC21K2073 to Colorado State University. (*Corresponding author: Chandrasekar Radhakrishnan.*)

Chandrasekar Radhakrishnan is with the The Cooperative Institute for Research in the Atmosphere, Colorado State University, Fort Collins, CO 80523 USA (e-mail: chandrasekar.radhakrishnan@colostate.edu).

V. Chandrasekar and Steven C. Reising are with the Department of Electrical and Computer Engineering, Colorado State University, Fort Collins, CO 80523 USA (e-mail: chandra@colostate.edu; steven.reising@colostate.edu).

Wesley Berg is with the Department of Atmospheric Science, Colorado State University, Fort Collins, CO 80523 USA (e-mail: wesley.berg@colostate.edu).

Shannon T. Brown is with the Jet Propulsion Laboratory, California Institute of Technology, Pasadena, CA 91109 USA (e-mail: shannon.t.brown@jpl.nasa.gov).

Digital Object Identifier 10.1109/JSTARS.2023.3303025

This work is licensed under a Creative Commons Attribution-NonCommercial-NoDerivatives 4.0 License. For more information, see https://creativecommons.org/licenses/by-nc-nd/4.0/

Radhakrishnan et. al. [2] (JSTARS, 2023)

Physical Cross Validation between TEMPEST-D and GPM-DPR Observations over Hurricane Delta on Oct. 7, 2020

Jet Propulsion Laboratory
California Institute of Technology

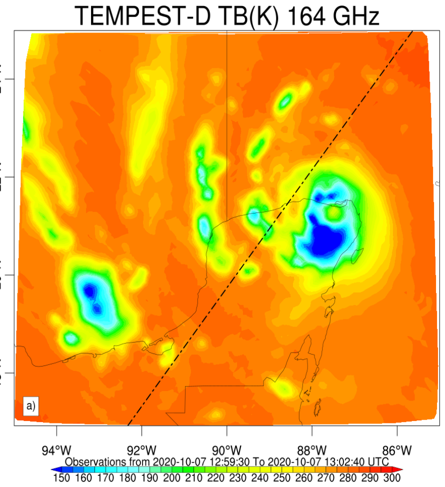

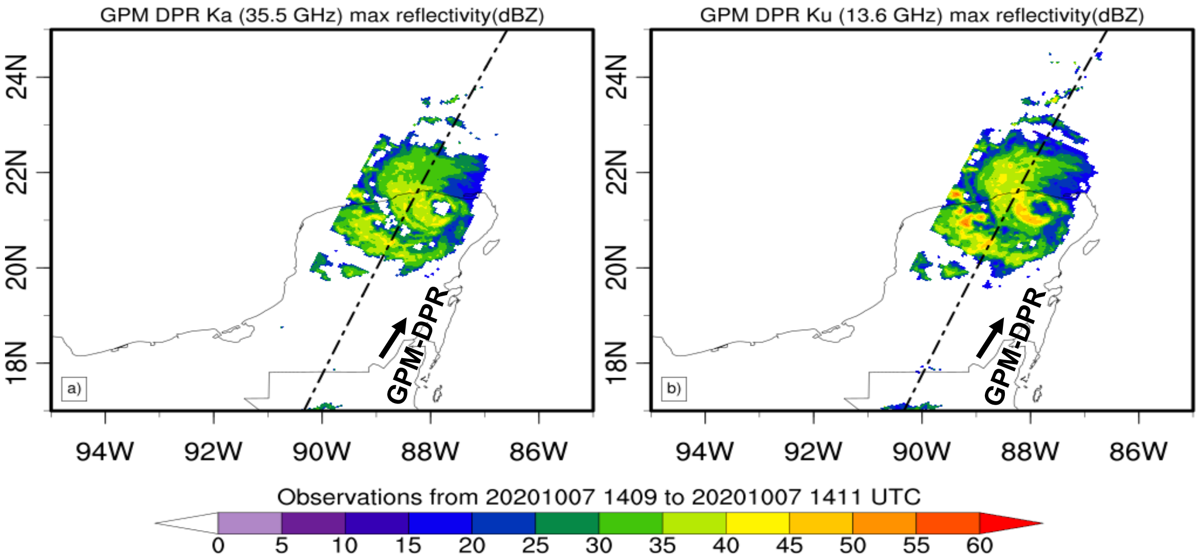

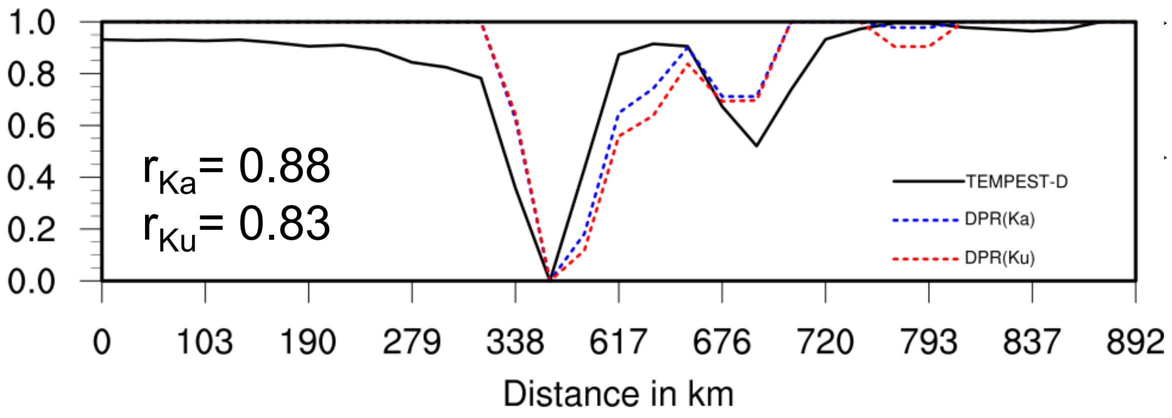

- **TEMPEST-D TB observations are normalized between 0 to 1.**
- **GPM-DPR reflectivity profile measurements are vertically cumulative, normalized between 0 and 1, and then flipped (Subtracted from 1)**

Synergy between Radar and Radiometer Observations of Precipitation from Space

V. Chandrasekar[1], Steven C. Reising[1], and Chandrasekar Radhakrishnan[1]
[1]Electrical and Computer Engineering, Colorado State University, Fort Collins, USA, chandra@colostate.edu

***Abstract*— This paper is a tribute to Prof Frank Marzano's legacy. The objective of this study is to cross-validate radar (active sensor) and radiometer (passive sensor) satellite observations over tropical cyclones, typhoons and hurricanes. To accomplish this, Global Precipitation Measurement (GPM) Dual-frequency Precipitation Radar (DPR) observations are compared with GPM Microwave Imager (GMI) and Temporal Experiment for Storms and Tropical Systems Demonstration (TEMPEST-D) CubeSat observations over precipitating systems. The purpose of this paper is twofold: first, to demonstrate a methodology to show consistency between DPR and GMI, and second, to apply this method to demonstrate consistency between DPR and TEMPEST-D CubeSat observations. This paper also develops a Pearson correlation coefficient (r) metric between parameters derived from radar and radiometer observations. The corresponding correlation between DPR and GMI, as well as between TEMPEST-D and DPR, are 0.90 and 0.85, respectively.**

***Index Terms*—GPM-GMI, GPM-DPR, TEMPEST-D, CubeSat, microwave radiometry, radar, instrument calibration.**

I. Introduction

Global weather satellite measurements are essential to observe and monitor the Earth, especially over the oceans where limited or no ground weather observations are available. Space-borne radiometer and radar observations provide critical information to initialize numerical weather prediction (NWP) models and improve prediction skills [1]. Microwave radiometers on weather satellites are passive sensors that capture upwelling radiation emitted from the Earth's surface and atmosphere, after interaction with atmospheric cloud liquid water, cloud ice water, and hydrometeors. The captured microwave radiation has information about the vertical column of the atmosphere. Radars on weather satellites are active sensors that measure the backscatter of microwave signals at different altitudes. The consistency between active and passive microwave sensors needs to be evaluated before generating combined weather observations to utilize the advantages of both sensors. A cross-comparison study between TEMPEST-D CubeSat and RainCube (Radar in a CubeSat) observations over precipitation systems showed high correlation between TEMPEST-D brightness temperatures (TB) and RainCube reflectivity profiles [2]. That study was conducted with nine storm events from around the globe. This study compares the GPM-DPR reflectivity observations with radiometer observations from the traditional GPM-GMI and a low-cost TEMPEST-D CubeSat over a hurricane system.

II. GPM and TEMPEST-D

The Global Precipitation Measurement (GPM) satellite mission is very successful, following the Tropical Rainfall Measuring Mission (TRMM). Both TRMM and GPM have been jointly developed by the National Aeronautics and Space Administration (NASA) and the Japan Aerospace Exploration Agency (JAXA). GPM is a low-Earth orbiting (LEO) satellite with a GPM Microwave Imager (GMI) and Dual-frequency Precipitation Radar (DPR). GMI has a 13-channel radiometer, and DPR has Ka-band (35.6 GHz) and Ku-band (10.5 GHz) vertically-pointing radars. This study used version 7 calibrated GMI TB data products at 13 km spatial resolution and the DPR data product at 5 km spatial resolution. The detailed GMI and DPR instrument configuration and specifications are described in [3,4]. TEMPEST-D is 6U CubeSat jointly developed by Colorado State University (CSU) and NASA/JPL. TEMPEST-D is a CubeSat demonstration mission for a future TEMPEST constellation [5] that aims to deploy six identical CubeSats in the same orbit with about 6 minutes separation between satellites. TEMPEST-D is a highly successful CubeSat mission that operated for nearly three years in orbit and provided high-quality global atmospheric observations, including of severe weather events over oceans and land. The TEMPEST-D radiometers measure at five millimeter-wave frequencies (87, 164, 174, 178, and 181 GHz) that provide detailed information on convection as well as the surrounding water vapor environment. At nadir the spatial resolution is 25 km for 87 GHz and 12.5 km for other four frequencies. TEMPEST-D instrument configuration and pre-launch calibration are described in [6]. The on-orbit validation of TEMPEST-D using the GPM-GMI and Microwave Humidity Sounder (MHS) instruments is discussed in [7].

III. Methodology

Figure 1 shows the flow chart of the cross-comparison procedure followed in the study. The first part of the study focuses on comparing the GMI and DPR observation over the precipitation events. The second part compares the observations from TEMPEST-D CubeSat and GPM-DPR. Only nadir observations from GMI and DPR overpasses are used in this study to reduce the complexity of analysis. The GMI and TEMPEST-D radiometers' radiances are from the

V. Chandrasekar et. al. [3] (EuCAP 2023)

Rainfall Estimation From TEMPEST-D CubeSat Observations over CONUS

- In prior research, a Machine Learning (ML) model was developed to estimate surface rain rate using TEMPEST-D observations within the CONUS region.

- The TEMPEST-D Brightness Temperatures (TBs) at five frequencies were employed as input, and the Multi-Radar Multi-Sensor (MRMS) Quantitative Precipitation Estimation (QPE) product was utilized as the ground truth or target for the ML model.

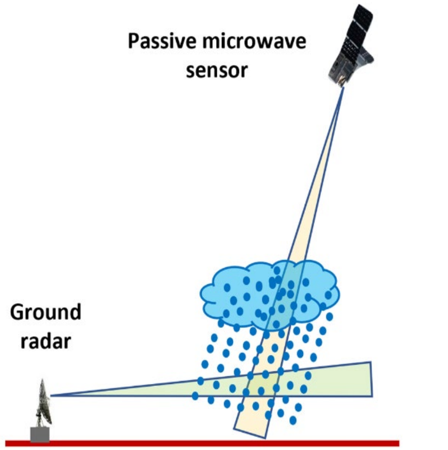

Graphical representation of rainfall measurement from ground-based weather radar and a space-borne passive microwave sensor.

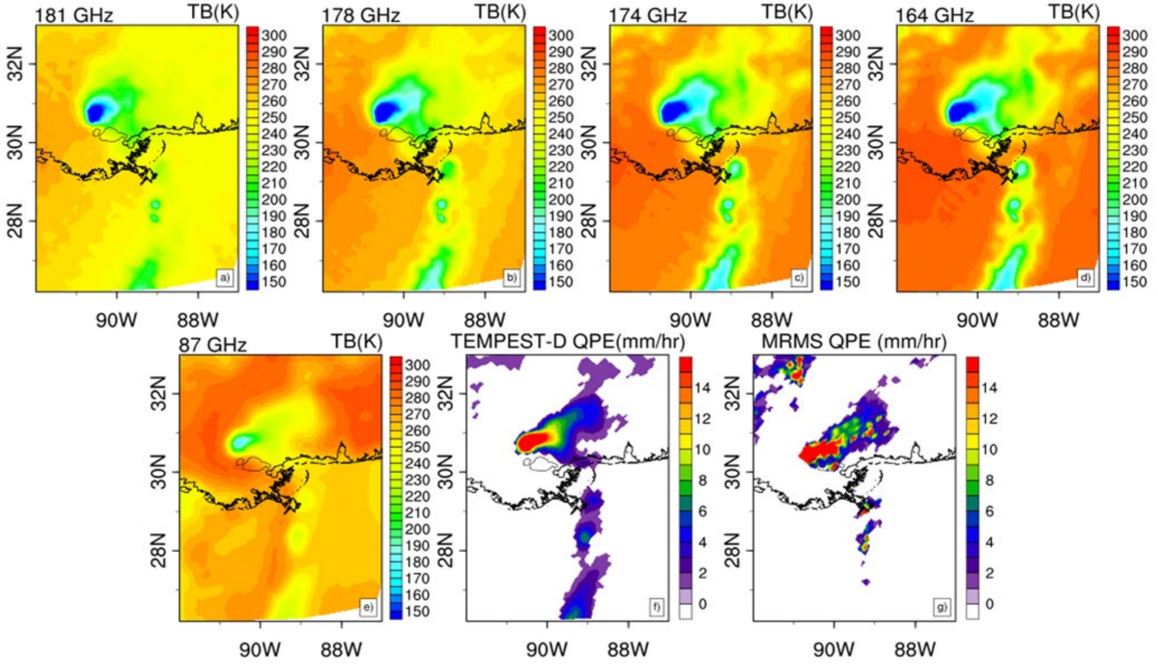

(a)–(e) TEMPEST-D TB observations of Tropical Storm Olga over New Orleans, Louisiana on October 26, 2019 at 09:00 UTC, (f) TEMPEST-D estimated rain rate, and (g) MRMS rain rate.

3626 IEEE JOURNAL OF SELECTED TOPICS IN APPLIED EARTH OBSERVATIONS AND REMOTE SENSING, VOL. 15, 2022

Rainfall Estimation From TEMPEST-D CubeSat Observations: A Machine-Learning Approach

Chandrasekar Radhakrishnan, V. Chandrasekar, *Fellow, IEEE*, Steven C. Reising, *Senior Member, IEEE*, and Wesley Berg

***Abstract*—In this study, a machine-learning model was used to produce surface rainfall estimates from Temporal Experiment for Storms and Tropical Systems – Demonstration (TEMPEST-D) microwave radiance observations from a CubeSat. The machine-learning model is based on an artificial neural network (ANN). The space-borne TEMPEST-D sensor performed brightness temperature (TB) observations at five frequencies (i.e., 87, 164, 174, 178, and 181 GHz) during its nearly three-year mission. The TEMPEST-D TBs were used as inputs, and the multiradar/multisensor system (MRMS) radar-only quantitative precipitation estimation product at the surface was used as the ground truth to train the ANN model. A total of 19 storms were identified that were simultaneously observed by TEMPEST-D and ground weather radar over the contiguous United States. The training dataset used 14 of the 19 storm cases. The other five storm cases, consisting of three continental storms and two land-falling hurricanes, were used for independent testing. A spatial alignment algorithm was developed to align the TEMPEST-D observed storm with the ground radar measurement of the storm. This study showed that the TEMPEST-D TBs captured storm features as well as current-generation satellite sensors, such as the global precipitation mission microwave imager. The results of this study demonstrated that the rainfall estimated from TEMPEST-D matches well with the MRMS surface rainfall product in terms of rainfall intensity, area, and precipitation system pattern. The average structural similarity index measure score for the five independent test cases is 0.78.**

***Index Terms*—Artificial neural network (ANN), cubeSats, machine learning, multiradar/multisensor system (MRMS), quantitative precipitation estimation (QPE), smallsats, temporal experiment for storms and tropical systems – demonstration (TEMPEST-D).**

I. INTRODUCTION

THE accurate estimation of surface rainfall is essential for numerous weather and climate applications over both land and ocean. The knowledge of precipitation intensity and its spatiotemporal variability helps to understand the climatology of precipitation. In addition, precipitation is an essential global and climatic variable [1] and it is critical to systems that support life on earth. Over land, precipitation is a primary source of fresh water. Monitoring and measurement of precipitation patterns have substantial economic value for the agriculture and forestry [2]. Precipitation also plays a vital role in removing particulate matter from the atmosphere [3]. For these reasons, an extensive infrastructure of ground-based instruments (rain gauges [4] and weather radars [5]) and space-borne weather sensors [6] has been developed to accurately measure the spatiotemporal variability of precipitation on both regional and global scales. The significant spatial and temporal variability of precipitation makes it difficult to measure with high accuracy across multiple scales; dense observational networks are required to capture the variability of precipitation, particularly at fine spatial and temporal scales. Ground-based rain gauge networks collect direct measurements of surface rainfall and provide high temporal resolution observations. However, they provide insufficient spatial coverage to estimate rainfall over larger areas. Kidd *et al.* [7] reported that only 0.000000000593% of earth's surface is covered by ground-based rain gauges.

Ground-based weather radars form the key infrastructure to monitor storms, issue watches, and warnings, as well as provide data for numerical weather prediction (NWP). In addition to these benefits, weather radars provide precipitation estimates over large areas (7000–32 000 km^2) with high spatial and temporal resolution and reasonable accuracy at that scale. Ground-based weather radar networks are currently in use throughout the U.S. and some other parts of the world, providing accurate rainfall measurements within the radar network's area of coverage. However, current radar networks primarily observe rainfall over land. A limited number of radars also perform observations over coastal zones. Some limitations of ground-based weather radars are as follows: Rainfall products from weather radars have larger uncertainties over complex terrain; and they lack coverage over the oceans. Oceanic rainfall is essential for understanding the global water cycle as well as providing critical information to initialize NWP models for the accurate forecasting of severe weather events, such as hurricanes and tropical cyclones [8], [9].

Satellite-based precipitation observations can be used to provide global coverage, particularly over the ocean and in the polar regions. Currently, operational weather satellites are deployed in both geostationary orbit (GEO) and low earth orbit (LEO). Weather satellites in GEO orbits, approximately 36 000 km

Manuscript received December 30, 2021; revised February 27, 2022 and March 28, 2022; accepted April 12, 2022. Date of publication April 27, 2022; date of current version May 16, 2022. This work was supported by the NASA Earth Venture Technology Demonstration Program under Grant NNX15AP56G, Grant 80NSSC20K1124, and Grant 80NSSC21K2073 to Colorado State University. *(Corresponding author: Chandrasekar Radhakrishnan.)*

Chandrasekar Radhakrishnan is with the Cooperative Institute for Research in the Atmosphere, Colorado State University, Fort Collins, CO 80523 USA (e-mail: chandrasekar.radhakrishnan@colostate.edu).

V. Chandrasekar and Steven C. Reising are with the Department of Electrical and Computer Engineering, Colorado State University, Fort Collins, CO 80523 USA (e-mail: chandra@colostate.edu; steven.reising@colostate.edu).

Wesley Berg is with the Department of Atmospheric Science, Colorado State University, Fort Collins, CO 80523 USA (e-mail: wesley.berg@colostate.edu).

Digital Object Identifier 10.1109/JSTARS.2022.3170835

This work is licensed under a Creative Commons Attribution 4.0 License. For more information, see https://creativecommons.org/licenses/by/4.0/

Radhakrishnan et. al. [4] (JSTARS, 2022)

Rainfall Estimation From TEMPEST-D Observations on a Global Basis

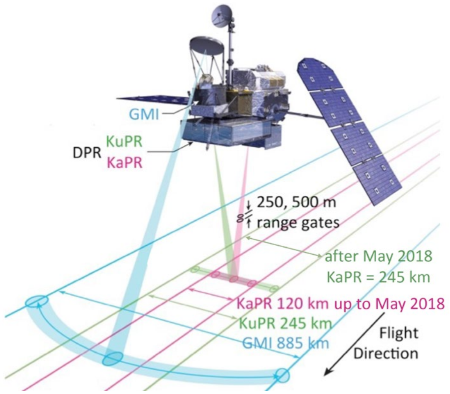

Scanning patterns and coverage of the GPM Core Observatory's GMI and DPR instruments.

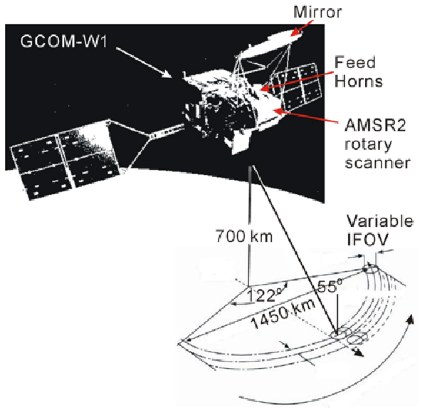

JAXA GCOM-W1 satellite and AMSR2 sensor illustrating earth surface scanning geometry

- The ML model was developed using TEMPEST-D TB observations over the period from 2018 to 2021.
- For the GMI-based ML model, the GPM GMI (GPROF) Radiometer Precipitation Profiling L2A (V07) dataset for each orbit with 13 km spatial resolution was utilized as a reference.
- Similarly, for the AMSR2-based ML model, the AMSR2 on GCOM-W1 (GPROF) Radiometer Precipitation Profiling L2A (V07) dataset with 10 km spatial resolution served as reference.
- For cross-comparison purposes, the GPM IMERG Early Precipitation L3 (V06) dataset with a spatial resolution of 0.1 x 0.1 degrees was utilized.

Image source:
https://gpm.nasa.gov/missions/GPM
https://www.scirp.org/pdf/IJG_2015011913083540.pdf

Data Pre-Processing and Database Creation for Machine Learning Model

- After conducting a spatiotemporal match (with a spatial resolution of 25 km and a temporal resolution of 5 minutes), we collected **750,000** overlapping data points between TEMPEST-D and GMI measurements, and **4.36 million** overlapping data points between TEMPEST-D and AMSR2 measurements.

- **Approximately 89% of the data falls below the light rain category, while 10% of the data corresponds to medium rain.**

- **Less than 1% of the data is classified as heavy rain. This poses a challenge for machine learning models attempting to identify and accurately estimate the intensity of heavy rain.**

	Rain Categories	Rain rate range	Percentage in GMI Database	Percentage in AMSR2 Database
1	No rain	< 0.1 mm/hr	48.69	49.17
2	Light Rain	0.1 <= RR < 2.5 mm/hr	38.75	40.62
3	Medium Rain	2.5 <= RR < 10 mm/hr	11.67	9.56
4	Medium Heavy Rain	10 <= RR < 20 mm/hr	0.70	0.54
5	Heavy Rain	20 mm/hr >= RR	0.17	0.08

Machine Learning (ML) based Rainfall Estimation Model

- Utilizing a hybrid approach combining precipitation identification and regression-based machine learning systems proves highly effective for addressing such problems [5].

- An ML classification model was developed to classify TEMPEST-D observations into categories of non-raining, light, medium, heavy, and extremely heavy rain conditions.

- **Additionally, four distinct Random Forest (RF) regression models were trained for the light, medium, medium heavy, and heavy rain categories.**

- **During the estimation phase, the process consists of two steps.** Firstly, the RF classification model determines the rain categories based on TEMPEST-D TB observations. Subsequently, in the second step, the RF regression models specific to each category are applied to the corresponding identified rain category to estimate the surface rain rate.

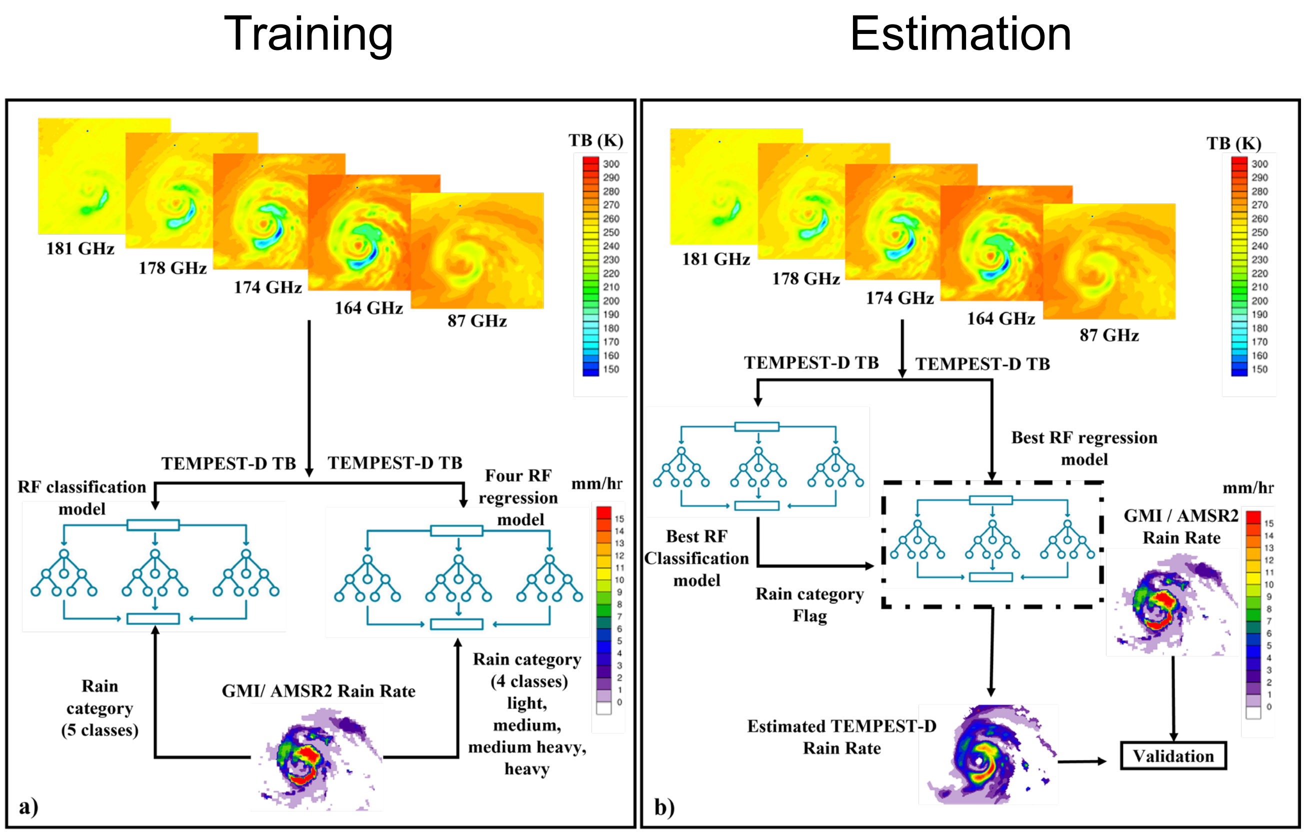

Independent Validation of TEMPEST-D Rain Rate Estimation System over Hurricane Dorian - 1

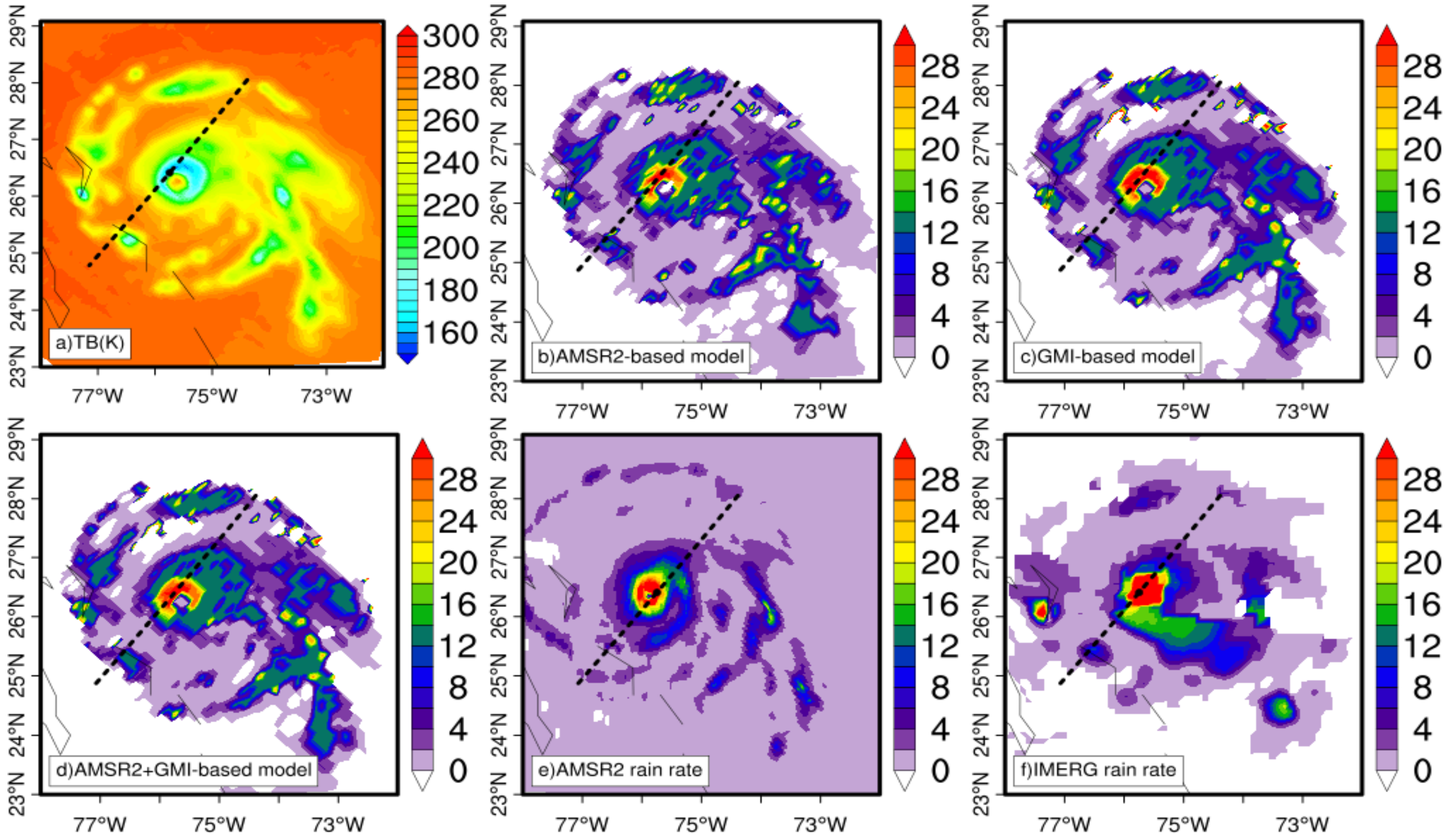

TEMPEST-H8 observations and estimated rain rates (mm/hr) (a) Brightness temperature (K) at 165 GHz. (b) AMSR2-based model. (c) GMI-based model. (d) Combined AMSR2 and GMI based model. (d) AMSR2 rain rate product (mm/hr) (e) IMERG rain rate (mm/hr)

- TEMPEST-D observed Hurricane Dorian on September 5, 2019, from 6:01 to 6:04 UTC, whereas AMSR2 observed it from 7:02 to 7:05 UTC. There is an approximate 1-hour time difference, with TEMPEST-D observations preceding those of AMSR2.
- For comparison, the IMERG product at 6:00 UTC on September 5, 2019, is utilized.

Independent Validation of TEMPEST-D Rain Rate Estimation System over Hurricane Dorian - 2

Comparison of estimated rain rates from TEMPEST-D observations using three ML models with AMSR2 and IMERG rain rate products.

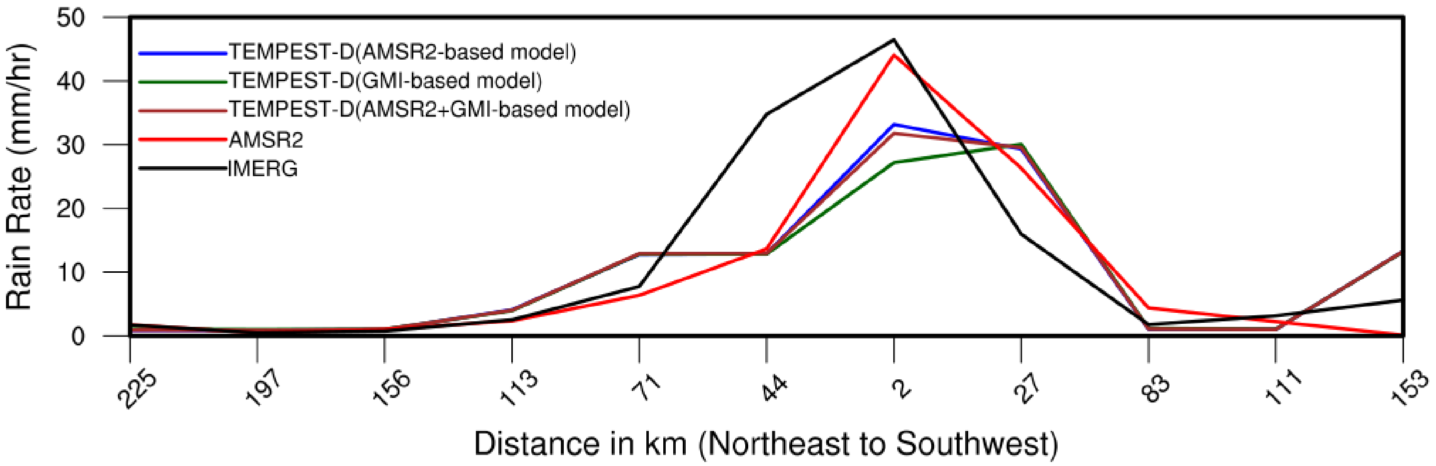

Comparison of AMSR2 and IMERG rain rate

	r	MAE (mm/hr)
AMSR2 vs IMERG	0.87	4.0

Comparison of TEMPEST-D and AMSR2 rain rate

TEMPEST -D vs AMSR2	*r*	MAE (mm/hr)
AMSR2-based Model	0.91	3.8
GMI-based Model	0.86	4.4
AMSR2+GMI-based Model	0.90	4.0

Comparison of TEMPEST-D and IMERG rain rate

TEMPEST-D vs IMERG	*r*	MAE (mm/hr)
AMSR2-based Model	0.79	6.1
GMI-based Model	0.73	6.7
AMSR2+GMI-based Model	0.78	6.2

r -> Correlation coefficient

Rain Rate Estimation from TEMPEST STP-H8 Observations over Hurricane Hilary - 1

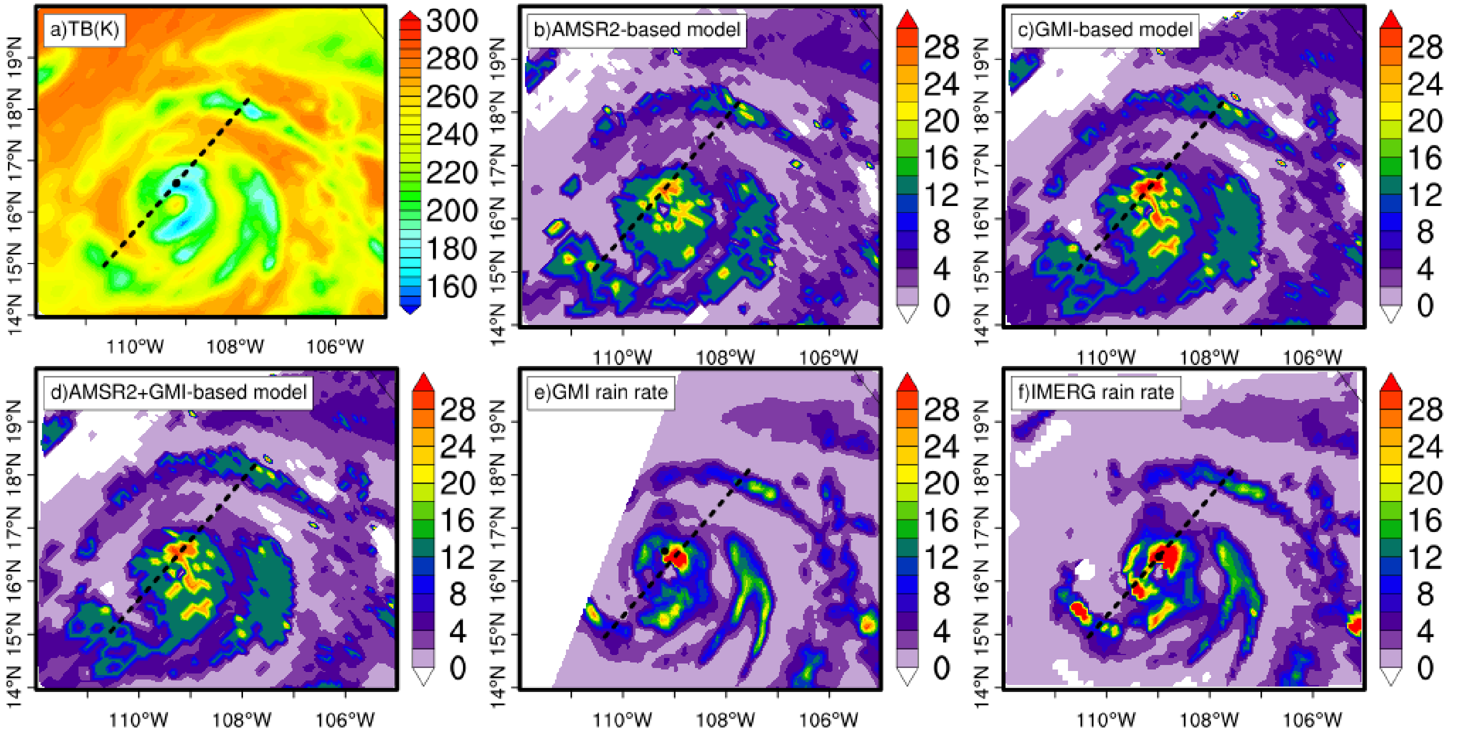

TEMPEST-H8 observations and estimated rain rates (mm/hr) (a) Brightness temperature (K) at 165 GHz. (b) AMSR2-based model. (c) GMI-based model. (d) Combined AMSR2 and GMI based model. (d) GMI rain rate product (mm/hr) (e) IMERG rain rate (mm/hr)

- TEMPEST STP-H8 observed Hurricane Hilary on August 17, 2023, from 21:52 to 21:56 UTC, while GMI observed it from 21:35 to 21:38 UTC. The time difference is approximately 17 minutes, with GMI ahead of TEMPEST STP-H8.

- For comparison, the IMERG product at 22:00 UTC on August 17, 2023, is utilized.

Rain Rate Estimation from TEMPEST STP-H8 Observations over Hurricane Hilary - 2

Comparison of estimated rain rates from TEMPEST-D observations using three ML models with GMI and IMERG rain rate products.

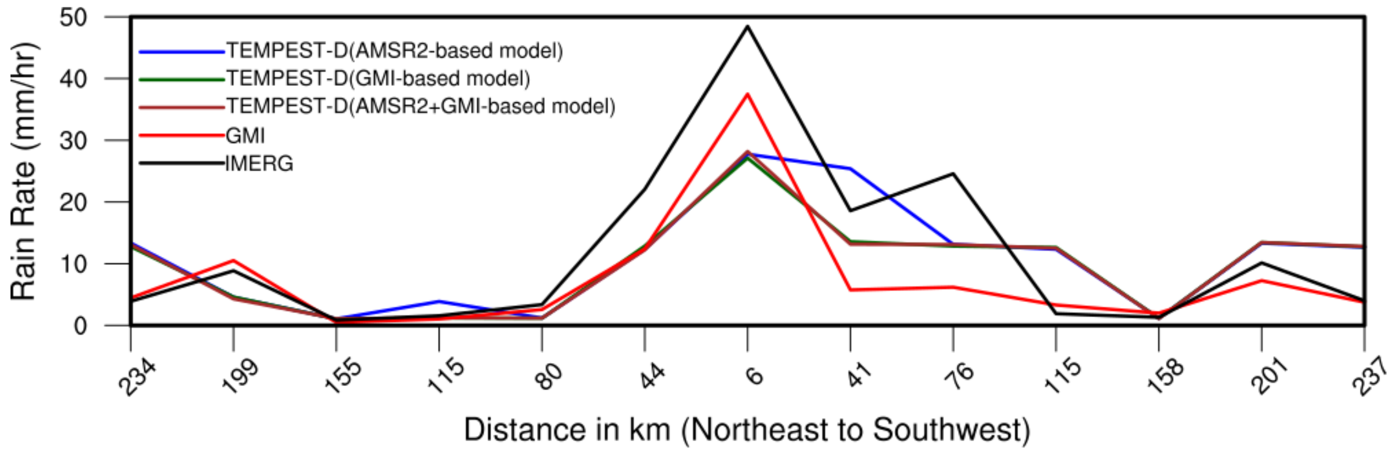

Comparison of TEMPEST STP-H8 and IMERG rain rate

TEMPEST STP-H8 vs IMERG	*r*	MAE (mm/hr)
AMSR2-based Model	0.76	6.8
GMI-based Model	0.80	6.6
AMSR2+GMI-based Model	0.80	6.6

Comparison of TEMPEST STP-H8 and GMI rain rate

TEMPEST STP-H8 vs GMI	*r*	MAE (mm/hr)
AMSR2-based Model	0.66	6.2
GMI-based Model	0.77	5.1
AMSR2+GMI-based Model	0.78	5.1

Comparison of GMI and IMERG rain rate

	r	MAE (mm/hr)
GMI vs IMERG	0.90	4.7

Summary and Conclusions - 1

- The main advance of this research is demonstration of a classification and quantification system using machine learning for rain rate estimation from passive microwave observations by small satellites.

- These integrated ML systems demonstrate superior performance in identifying heavy rainfall pixels and accurately estimating intense precipitation compared to methods based solely on regression.

- Independent validations demonstrate consistent performance across all three ML systems when compared with IMERG rain rate products, showing an average correlation coefficient (*r*) of 0.79 and an average MAE of 5.6 mm/hr, indicating strong agreement with IMERG estimates.

Summary and Conclusions - 2

- The high-quality rain rate estimates from TEMPEST-H8 TB observations over tropical cyclone systems demonstrated that the developed ML systems perform well in estimating rain rates from various sensors with similar channel characteristics, with an average correlation coefficient (*r*) of 0.81 and an average MAE of 7.0 mm/hr.

- The performance of the ML system is similar while using TEMPEST-D and TEMPEST-H8 TB observations.

References

[1] S. C. Reising, T. C. Gaier, S. Padmanabhan, B. H. Lim, C. Heneghan, C. D. Kummerow, W. Berg, V. Chandrasekar, C. Radhakrishnan, S. T. Brown, J. Carvo, and M. Pallas, “An Earth Venture In-Space Technology Demonstration Mission for Temporal Experiment for Storms and Tropical Systems (TEMPEST),” *Proc. 2018 IEEE International Geoscience and Remote Sensing Symposium (IGARSS 2018)*, pp. 6301-6303, 2018.

[2] C. Radhakrishnan, V. Chandrasekar, S. C. Reising, W. Berg and S. T. Brown, “TEMPEST-D and GPM-GMI Observations Over Precipitating Systems: A Cross-Validation Study,” *IEEE Journal of Selected Topics in Applied Earth Observations and Remote Sensing*, vol. 16, pp. 7422-7432, 2023.

[3] V. Chandrasekar, S. C. Reising and C. Radhakrishnan, “Synergy between Radar and Radiometer Observations of Precipitation from Space,” *2023 17th European Conference on Antennas and Propagation (EuCAP)*, Florence, Italy, 2023, pp. 1-4, doi: 10.23919/EuCAP57121.2023.10133341.

[4] C. Radhakrishnan, V. Chandrasekar, S. C. Reising and W. Berg, “Rainfall Estimation from TEMPEST-D CubeSat Observations: A Machine-Learning Approach,” *IEEE Journal of Selected Topics in Applied Earth Observations and Remote Sensing*, vol. 15, pp. 3626-3636, 2022.

[5] H. Liu, V. Chandrasekar and E. Gorgucci, "Detection of rain/no rain condition on the ground based on radar observations," *IEEE Transactions on Geoscience and Remote Sensing*, vol. 39, pp. 696-699, 2001.

Thank you

Independent Validation over Hurricane Florence

- TEMPEST-D observations over Hurricane Florence on September 9, 2018, from 11:48 to 11:52 UTC are utilized.
- For comparison, the IMERG product at 12:00 UTC on September 9, 2018, is employed.

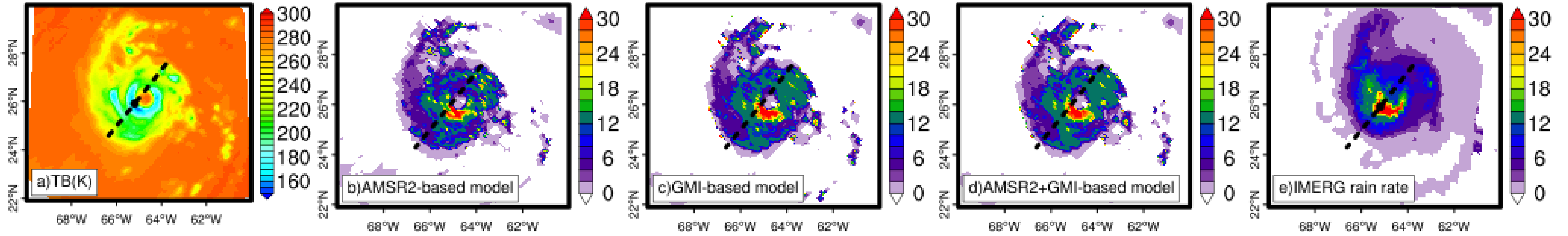

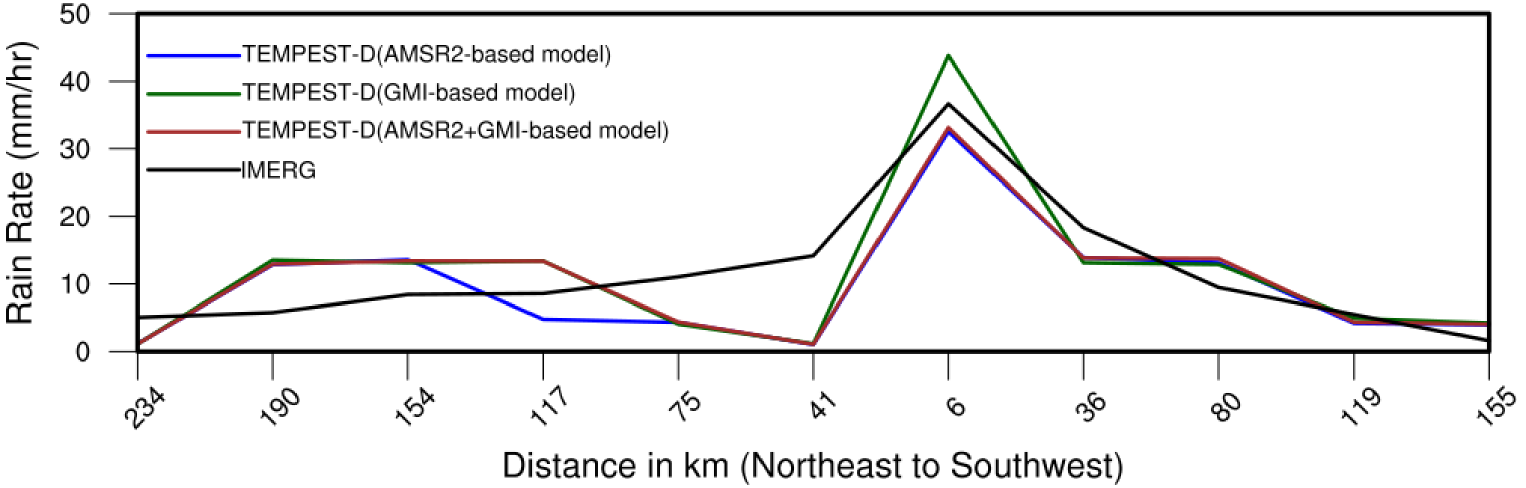

TEMPEST-D vs IMERG	*r*	MAE (mm/hr)
AMSR2-based Model	0.80	5.0
GMI-based Model	0.83	5.4
AMSR2+GMI-based Model	0.79	5.1

Rain Rate Estimation from TEMPEST STP-H8 Observations over Tropical Cyclone Batsirai - 1

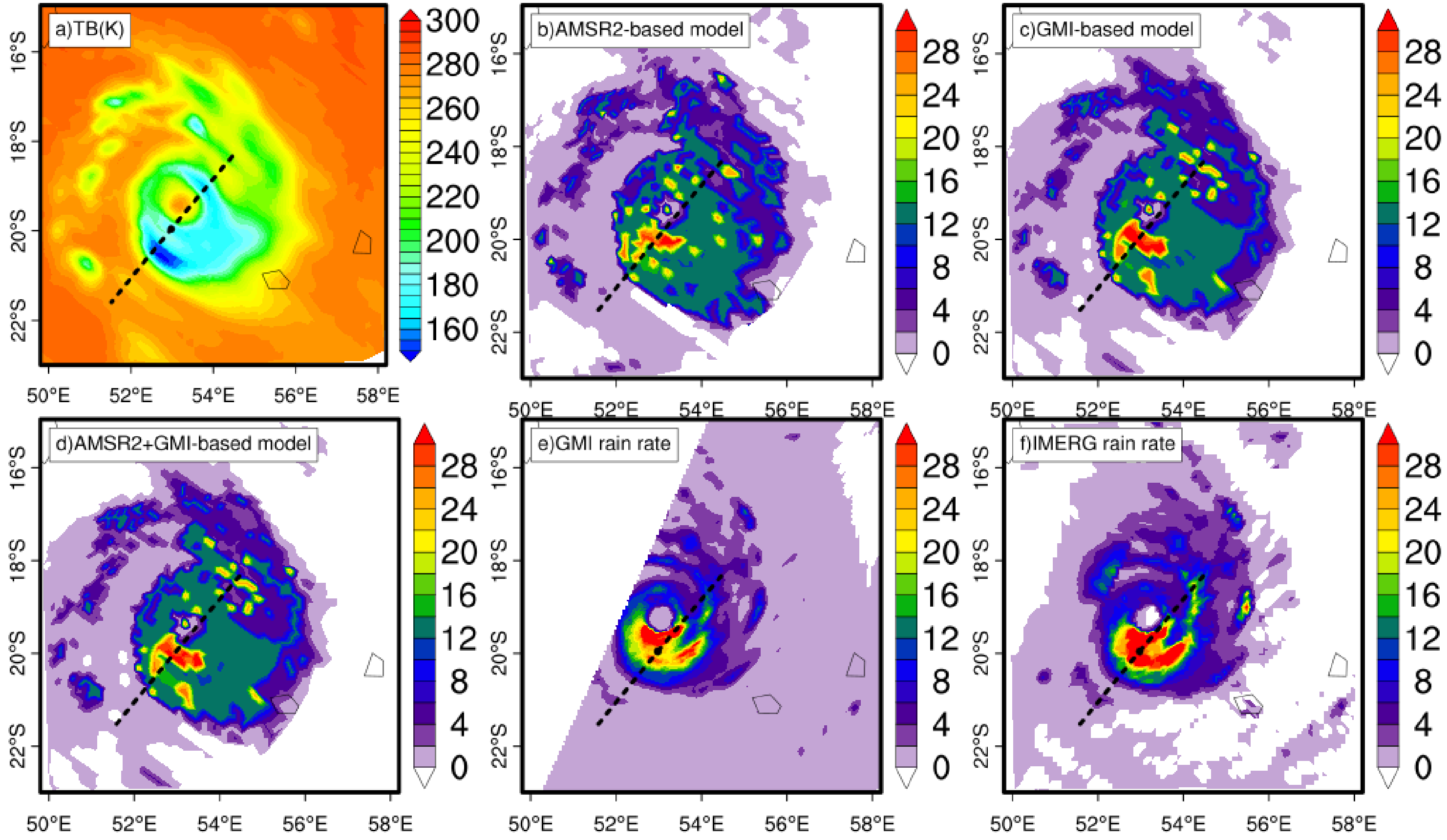

TEMPEST-H8 observations and estimated rain rates (mm/hr) (a) Brightness temperature (K) at 165 GHz. (b) AMSR2-based model. (c) GMI-based model. (d) Combined AMSR2 and GMI based model. (d) GMI rain rate product (mm/hr) (e) IMERG rain rate (mm/hr)

- TEMPEST STP-H8 observed Tropical Cyclone Batsirai on February 4, 2022, from 05:09 to 05:12 UTC, while GMI observed it from 05:26 to 05:28 UTC. The time difference is approximately 17 minutes, with GMI ahead of TEMPEST STP-H8.
- For comparison, the IMERG product at 05:00 UTC on February 4, 2022, is utilized.

Rain Rate Estimation from TEMPEST STP-H8 Observations over Tropical Cyclone Batsirai - 2

Comparison of estimated rain rates from TEMPEST-D observations using three ML models with GMI and IMERG rain rate products.

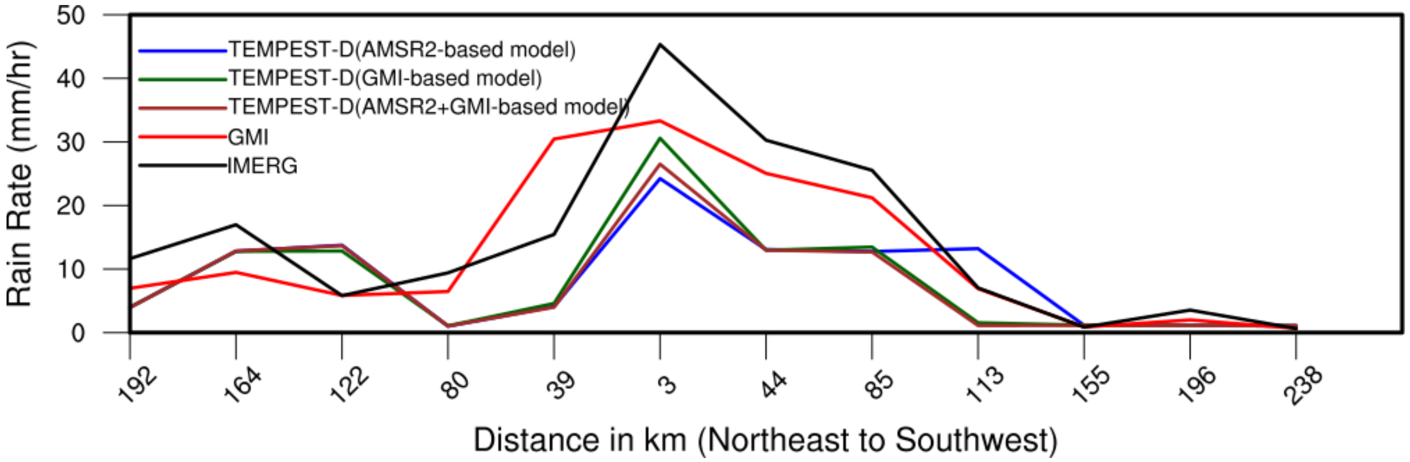

Comparison of TEMPEST STP-H8 and IMERG rain rate

TEMPEST STP-H8 vs IMERG	*r*	MAE (mm/hr)
AMSR2-based Model	0.78	7.7
GMI-based Model	0.88	7.0
AMSR2+GMI-based Model	0.86	7.5

Comparison of TEMPEST STP-H8 and GMI rain rate

TEMPEST STP-H8 vs GMI	*r*	MAE (mm/hr)
AMSR2-based Model	0.61	6.4
GMI-based Model	0.70	5.7
AMSR2+GMI-based Model	0.67	6.2

Comparison of GMI and IMERG rain rate

	r	MAE (mm/hr)
GMI vs IMERG	0.88	4.1

RF Classification Model Performance on Training and Testing Datasets

- Training used 80% of data points, and testing used 20% of data points.
- The AMSR2-based model used 3.48 million data points for training and 872,000 data points for testing.
- The GMI-based model used 600,000 data points for training and 150,000 data points for testing.
- The combined AMSR2 and GMI-based model used 4.08 million data points for training and 1.02 million data points for testing.

F1 scores from the three best RF classification models for each rain category on both the training and testing datasets

Rain Categories	AMSR2 based model		GMI based model		AMSR2 and GMI based model	
	Training	Testing	Training	Testing	Training	Testing
No Rain	0.85	0.81	0.78	0.75	0.77	0.74
Light Rain	0.64	0.55	0.54	0.47	0.57	0.48
Medium Rain	0.60	0.45	0.46	0.44	0.54	0.43
Medium Heavy Rain	0.67	0.53	0.43	0.35	0.59	0.45
Heavy Rain	0.83	0.73	0.65	0.57	0.73	0.62

RF Classification Model Performance on Training and Testing Datasets

Optimal parameters determined from grid search hyperparameter tuning process

RF Classification models	Number of estimators	Maximum depth	Minimum samples of leaf	Accuracy	
				Training	Testing
AMSR2 based model	40	10	2	0.72	0.62
GMI based model	20	6	3	0.58	0.53
AMSR2 and GMI based model	40	10	2	0.64	0.55

F1 scores from the three best RF classification models for each rain category on both the training and testing datasets

Rain Categories	AMSR2 based model		GMI based model		AMSR2 and GMI based model	
	Training	Testing	Training	Testing	Training	Testing
No Rain	0.85	0.81	0.78	0.75	0.77	0.74
Light Rain	0.64	0.55	0.54	0.47	0.57	0.48
Medium Rain	0.60	0.45	0.46	0.44	0.54	0.43
Medium Heavy Rain	0.67	0.53	0.43	0.35	0.59	0.45
Heavy Rain	0.83	0.73	0.65	0.57	0.73	0.62

RF Regression Model Performance on Training and Testing Datasets

Correlation coefficient values for rainfall for the best Machine learning (Randon Forest) models developed from three different datasets for four rain categories on both the training and testing datasets.

	Light Rain		Medium Rain		Medium Heavy Rain		Heavy Rain	
	Training	Testing	Training	Testing	Training	Testing	Training	Testing
AMSR2 based model	0.71	0.53	0.73	0.52	0.73	0.57	0.77	0.55
GMI based model	0.42	0.36	0.63	0.34	0.78	0.3	0.84	0.53
AMSR2 and GMI based model	0.7	0.37	0.68	0.40	0.70	0.47	0.81	0.54

AMSR2 and GMI Instrument Channels Frequencies and Spatial Resolution

AMSR2

Band [GHz]	Polarization	Spatial Resolution(3-dB footprint size)[km x km]
6.93	V,H	62 x 35
7.3	V,H	62 x 35
10.65	V,H	42 x 24
18.7	V,H	22 x 14
23.8	V,H	26 x 15
36.5	V,H	12 x 7
89	V,H	5 x 3

GMI

Band [GHz]	Polarization	Spatial Resolution(3-dB footprint size) [km x km]
10.65	V,H	32 x 19
18.7	V,H	18 x 11
23.8	V	16 x 10
36.5	V,H	15 x 9
89	V,H	7 x 4
165.5	V,H	6 x 4
183.31+/-3	V	6 x 4
183.31+/-7	V	6 x 4

TEMPEST-D and TEMEPST-H8 spatial resolution varies from 25 km at 87 GHz to 12.5 km at 164-181 GHz.